Oropouche virus glycoprotein topology and cellular requirements for virus-like particle assembly

Natalia S. Barbosa[a,b,c], Luis L. P. daSilva[a,b*], Colin M. Crump[c#], Stephen C. Graham[c#]

[a] Center for Virus Research, Ribeirão Preto Medical School, University of São Paulo, Ribeirão Preto, SP, Brazil

[b] Department of Cell and Molecular Biology, Ribeirão Preto Medical School, University of São Paulo, Ribeirão Preto, SP, Brazil

[c] Department of Pathology, University of Cambridge, Cambridge, United Kingdom

[#] Address correspondence to Colin M. Crump, cmc56@cam.ac.uk, or Stephen C. Graham, scg34@cam.ac.uk.

ORCIDs: 0000-0002-2926-5294 (NSB), 0000-0003-3558-0087 (LLPdS), 0000-0001-9918-9998 (CMC), 0000-0003-4547-4034 (SCG)

Running title: Virus-like particle assay for Oropouche virus

Keywords: Bunyavirus, Bunyamwera virus, polyprotein processing, virus budding

Author Contributions: Conceptualization: LLPdS, CMC, SCG; Funding Acquision: NSB, LLPdS, CMC, SCG; Investigation: NSB; Methodology: CMC, SCG; Resources: CMC, SCG; Supervision: LLPdS, CMC, SCG; Visualization: NSB, SCG; Writing – original draft: NSB, SCG; Writing – review & editing: NSB, LLPdS, CMC, SCG.

Word count: 5801 (Abstract: 238; Importance: 150)

Abstract

Oropouche virus (OROV; *Genus: Orthobunyavirus*) is the etiological agent of Oropouche fever, a debilitating febrile illness common in South America. To facilitate studies of OROV budding and assembly, we developed a system for producing OROV virus-like particles (VLPs). Using this system we show that the OROV surface glycoproteins Gn and Gc self-assemble to form VLPs independently of the non-structural protein NSm. Mature OROV Gn has two trans-membrane domains that are crucial for glycoprotein translocation to the Golgi complex and VLP production. Inhibition of Golgi function using the drugs brefeldin A and monensin inhibit VLP secretion, with monensin treatment leading to an increase in co-localisation of OROV glycoproteins with the *cis*-Golgi marker protein GM130. Infection studies have previously shown that the cellular Endosomal Sorting Complexes Required for Transport (ESCRT) machinery is recruited to Golgi membranes during OROV assembly and that ESCRT activity is required for virus secretion. We demonstrate that a dominant negative form of the ESCRT-associated ATPase VPS4 significantly reduces Gn secretion in our VLP assay. Proteasome inhibition using the drug MG132 also disrupts VLPs secretion, suggesting that ubiquitylation promotes ESCRT-mediated VLP release. Additionally, we observe co-localisation between OROV glycoproteins and a specific subset of fluorescently-tagged ESCRT-III components, providing the first insights into which ESCRT-III components are required for OROV assembly. Our *in vitro* assay for OROV VLP production has allowed us to define molecular interactions that promote OROV release and will facilitate future studies of orthobunyavirus assembly.

Importance

Oropouche virus is the etiological agent of Oropouche fever, a debilitating febrile illness common in South America. The tripartite genome of this zoonotic virus is capable of reassortment and there have been multiple epidemics of Oropouche fever in South America over the last 50 years, making Oropouche virus infection a significant threat to public health. However, the molecular characteristics of this arbovirus are poorly understood. We have developed an *in vitro* virus-like particle production assay for Oropouche virus, allowing us to study the assembly and release of this dangerous pathogen without high-containment biosecurity. We determined the polyprotein sites that are cleaved to yield the mature Oropouche virus surface glycoproteins and characterised the cellular machinery required for glycoprotein secretion. Our study provides important insights into the molecular biology of Oropouche virus infection, in addition to presenting a robust virus-like particle production assay that should facilitate future functional and pharmacological inhibition studies.

Introduction

Oropouche virus (OROV) is an arbovirus that is the etiological agent of Oropouche fever, a debilitating febrile illness. Oropouche fever symptoms range from high fever to vomiting, photophobia and, in rare cases, aseptic meningitis or meningoencephalitis (1). OROV is prevalent in the Caribbean and tropical regions of Latin America, and more than 30 epidemics of Oropouche fever have occurred since the first isolation of OROV in 1955 (1). Clinical diagnosis of Oropouche fever is challenging due to the resemblance of its symptoms to diseases caused by other arboviruses like Dengue virus, Zika virus and Chikungunya virus (2). There are no specific antiviral treatments for Oropouche fever, nor is there an effective vaccine to prevent OROV infection. The zoonotic origin, history of human spill-over, tri-segmented RNA genome that is capable of re-assortment (3) and increasing contact between humans and wild-animal reservoirs due to deforestation (1) make OROV a serious epidemic threat.

OROV belongs to *Orthobunyavirus* genus of the *Peribunyaviridae* family, one of the twelve families of the order *Bunyavirales*. Orthobunyaviruses form spherical enveloped virus particles that are 100–120 nm in diameter and orthobunyavirus genomes comprise three negative sense single-stranded RNA segments: The small segment (S) encodes the nucleocapsid N protein (25–30 kDa), which oligomerizes and encapsidates the viral genome, and the non-structural protein NSs; The medium segment (M) encodes a polyprotein that is post-translationally cleaved by host proteases to yield the viral surface glycoproteins (Gc and Gn) plus a non-structural protein NSm; The large segment (L) encodes the viral RNA dependent RNA polymerase (RdRp) that catalyzes viral replication and transcription. The viral RNA segments are encapsidated by the N protein to form a ribonucleoprotein complex that associates with both the RdRp and the surface glycoproteins to promote virus particle assembly (4). The Gn (~32 kDa) and Gc (~110 kDa) glycoproteins are integral membrane proteins with N-terminal ectodomains and they associate in the host endoplasmic reticulum (ER) before being transported to the Golgi complex, the main site of virion assembly (5-7). Studies with Bunyamwera virus (BUNV), the prototypical orthobunyavirus, have shown that the virus particles undergo distinct morphological changes inside Golgi and *trans*-Golgi network cisternae (6), and studies of both BUNV and OROV have shown profound fragmentation of Golgi complex cisternae during virus infection of some cell types (5, 6).

OROV assembly at the Golgi complex is stimulated by the cellular Endosomal Sorting Complexes Required for Transport (ESCRT) machinery (5). The ESCRT machinery mediates membrane deformation and scission in an ‘inside-out’ topology, in contrast to the ‘outside-in’ topology of endocytic vesicles (8). The human ESCRT machinery comprises multiple distinct protein complexes (ESCRT-0, ESCRT-I, ESCRT-II and ESCRT-III) plus several accessory proteins, with final membrane scission being promoted by the concerted action of ESCRT-III and the ATPase VPS4 (9). The ESCRT-III machinery is formed by members of the charged multivesicular body protein (CHMP) family, with distinct CHMP proteins playing specific coordinated roles. The first ESCRT-III component recruited is CHMP6, which recruits CHMP4 isotypes (CHMP4A or CHMP4B) to homo-oligomerizes at the target membrane. The CHMP2A plus CHMP3 complex and/or CHMP2B alone are then recruited, activating VPS4 to

promote ESCRT-III filament disassembly and membrane scission (9-11). Virus recruitment of the ESCRT-III machinery is canonically mediated by direct association of viral 'late domains' with ESCRT-I, the cellular ubiquitylation machinery and/or the accessory protein ALIX. These interactions culminate in recruitment and activation of the ESCRT-III machinery (12, 13). With the exception of flaviviruses, which recruit ESCRT components to the ER (14), most viruses recruit ESCRT machinery to the plasma membrane, endosomes or other 'post-Golgi' membranes (13, 15). It is therefore particularly interesting that OROV budding involves direct recruitment of ESCRT machinery to Golgi membranes (5). The OROV glycoproteins do not contain any identifiable viral 'late domains' and the molecular basis of ESCRT machinery recruitment by OROV thus remains to be established.

The study of virus assembly and budding is greatly aided by recombinant technology to generate virus-like particles (VLPs), which are released by cultured cells expressing specific virus components and are genome-free but otherwise structurally resemble authentic virus particles. Recombinant VLP systems facilitate investigation of highly-pathogenic virus assembly pathways under reduced biosafety containment (16, 17) and VLPs have been widely used as tools for vaccine development (18). VLP production systems have been established for several members of the order *Bunyavirales*, with phlebovirus and hantavirus VLP assembly requiring expression of the viral glycoproteins but not the nucleoprotein (19, 20). While a mini-replicon system has been reported for BUNV and OROV (21, 22), no VLP system has been established to study orthobunyavirus assembly and budding.

Here we report production of OROV VLPs via recombinant expression of the M polypeptide. We observe that the M polyprotein yields a mature Gn protein containing two transmembrane domains that are crucial for viral glycoprotein targeting to the Golgi complex and for VLP production. We show that pharmacological disruption of Golgi function prevents OROV VLP secretion, as does perturbation of ESCRT function, which highlights the utility of this VLP production assay for probing cellular determinants of OROV assembly. Finally, we show co-localisation of ESCRT components with Gn and Gc in cells, giving insights into the cellular factors that sustain OROV assembly and release.

Results

OROV virus-like particle characterization

The middle (M) segment of the OROV genome (residues 1–1420) was cloned as a cDNA fragment into the mammalian expression vector pcDNA3.1 with an HA epitope tag between the secretion signal sequence (SS) and the first residue of the mature Gn protein (Fig. 1A). Transfection of HEK293T cells with HA-tagged OROV M polyprotein yielded high levels of Gn and Gc (observed as bands at ~35 kDa and ~120 kDa, respectively) in the supernatant, consistent with the production of OROV virus-like particles (VLPs) by these transfected cells (Fig. 1B). In order to establish whether both OROV glycoproteins are required for VLP production, OROV Gn (M segment residues 1–312) and Gc (M segment residues 481–1420) were cloned separately into pcDNA3.1 with an N-terminal secretion signal and HA epitope tag (Fig. 1A), the polypeptide cleavage sites being inferred from homology with those determined or predicted for the Bunyamwera M polyprotein (23). As expected, neither Gn nor Gc was abundant in the cell supernatant when transfected into HEK293T cells in isolation. However, we also failed to observe secreted glycoproteins when the proteins were co-expressed (Fig. 1B). This was unexpected as a previous study of OROV infection had shown that the NSm polypeptide, which lies between Gn and Gc in the M polyprotein, was dispensable for virion production (24). Furthermore, we observed that HA-tagged Gn from cells transfected with a plasmid encoding HA-tagged M polypeptide migrated more slowly in SDS-PAGE than Gn from cells transfected with the HA-Gn plasmid (Fig. 1B), consistent with the two proteins having different masses. Analysis of the OROV M polypeptide sequence using the SignalP 5.0 server (25) suggested that the cleavage site which liberates Gn from the M polypeptide may lie between residues G335 and E336 (Fig. 1A, second arrow), thus yielding a mature Gn protein with two trans-membrane domains (TMDs). A second HA-tagged Gn expression construct that included this extra TMD was thus generated (GnX; residues 1-339). While GnX was not secreted into the medium following transfection on its own into HEK293T cells, both GnX and Gc were abundant in the supernatant of cells co-transfected with constructs encoding both proteins (Fig. 1C). This suggested that co-expression of Gc with GnX is sufficient to stimulate production of VLPs, VLP production requiring Gn to encompass the first two TMDs of the M polyprotein. To test whether the two TMDs plus cytosolic region of GnX (residues 203–339; GnCTX) were sufficient to promote Gc secretion, and thus VLP production, HEK293T cells were co-transfected with GnCTX and Gc expression constructs. Neither Gc nor GnCTX was secreted to the supernatant of these co-transfected cells, indicating that GnCTX is not sufficient to promote secretion of Gc (Fig. 1C). Taken together, these results demonstrate that OROV VLPs are formed following co-expression of the surface glycoproteins, either as individual proteins or as a polyprotein, but that the M polyprotein is cleaved after the second TMD to liberate the mature OROV Gn protein (GnX).

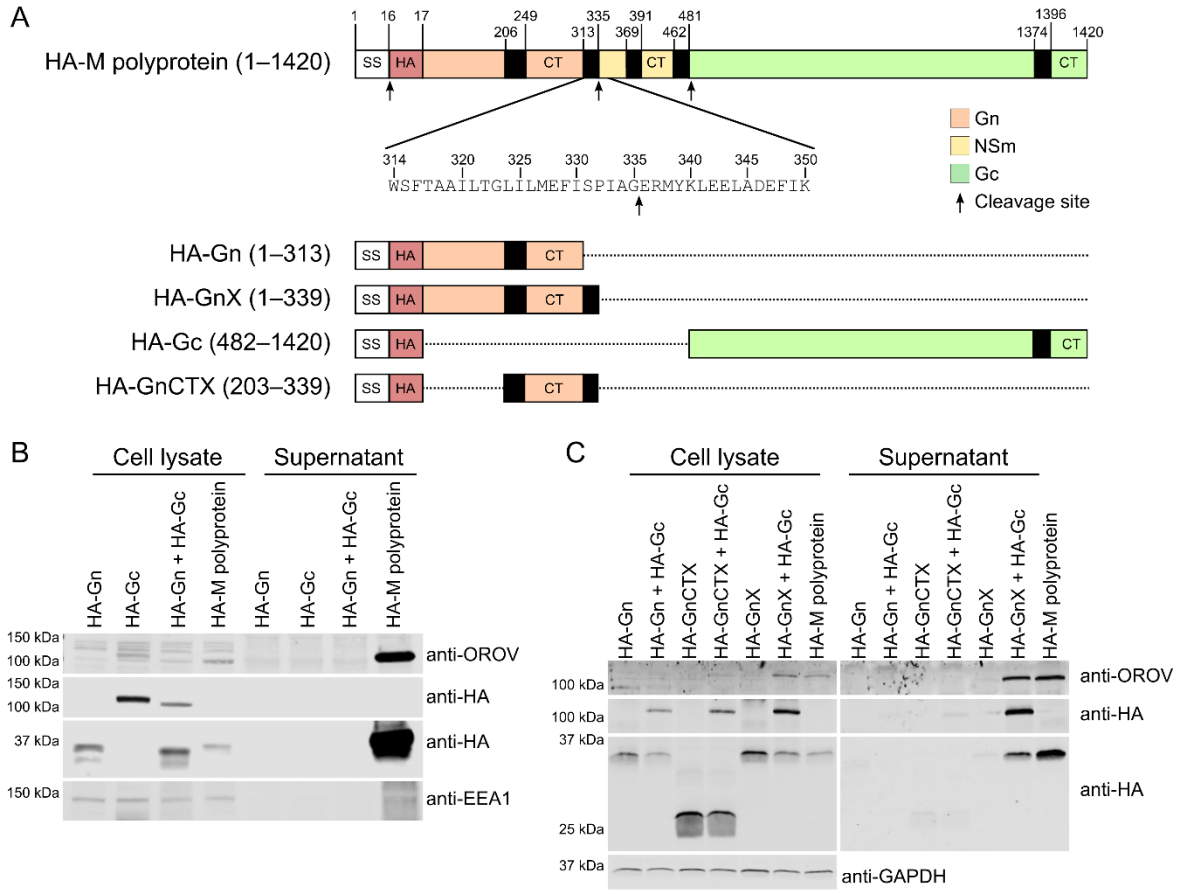

Figure 1. Recombinant production of OROV virus-like particles. (A) Schematic representation of the recombinant constructs used to express the OROV M polyprotein, individual glycoproteins or domains thereof. All expression constructs were preceded by the OROV M signal sequence (SS; unshaded) and an HA epitope tag (HA; red shading). Regions corresponding to Gn, Gc and the NSm non-structural protein are shaded in orange, green and yellow, respectively, with cytosolic tails denoted (CT). Predicted transmembrane regions (black) and polypeptide cleavage sites (arrows) are shown. (B and C) HEK293T cells were transfected with HA-tagged OROV M (poly)protein constructs. After 48 h cell lysates and supernatants were harvested, subjected to SDS-PAGE and immunoblotted using anti-HA and anti-OROV antibodies to detect secreted proteins, the latter polyclonal antibody detecting Gc but not Gn, and with anti-EEA1 (B) or anti-GAPDH (C) antibodies used as loading controls.

The GnX:Gc complex is sufficient for Golgi localization

During infection, the orthobunyavirus M segment is translated at the ER before the Gn and Gc proteins are transported to the Golgi apparatus, which is the main site of virus assembly (4). In order to investigate the subcellular distribution of recombinant OROV glycoproteins (Fig. 1A), HeLa cells were transfected with HA-tagged OROV glycoproteins and then stained for the HA signal and for the ER chaperone calnexin 2 (CNX2) or the *cis*-Golgi marker GM130 (Fig. 2). When expressed alone, HA-tagged Gn, Gc and GnX all co-localized with CNX2 at the ER and did not co-localise with GM130 at the Golgi (Fig. 2A–C). Similarly, when HA-tagged Gn and Gc were co-expressed they were retained at the ER and did not co-localise at the Golgi (Fig. 2D). However, when HA-tagged GnX and Gc were co-expressed they showed extensive co-localisation with GM130 at the Golgi and less-extensive co-localisation with CNX2 at the ER (Fig. 2E). Extensive GM130 co-localisation was also observed when

the HA-tagged OROV M polyprotein was expressed (Fig. 2F). Additionally, HA-stained punctae could often be observed outside cells expressing the M polyprotein (Fig. 2F), consistent with the production of VLPs that remain adhered to the coverslip during fixation and subsequent preparation of the microscope slides. Taken together, these data suggest that co-expression of Gn spanning the first two predicted TMDs (residues 1–339; GnX) with Gc, either as separate polypeptides or as a polyprotein, is necessary and sufficient for these proteins to be transported from the ER to the Golgi apparatus.

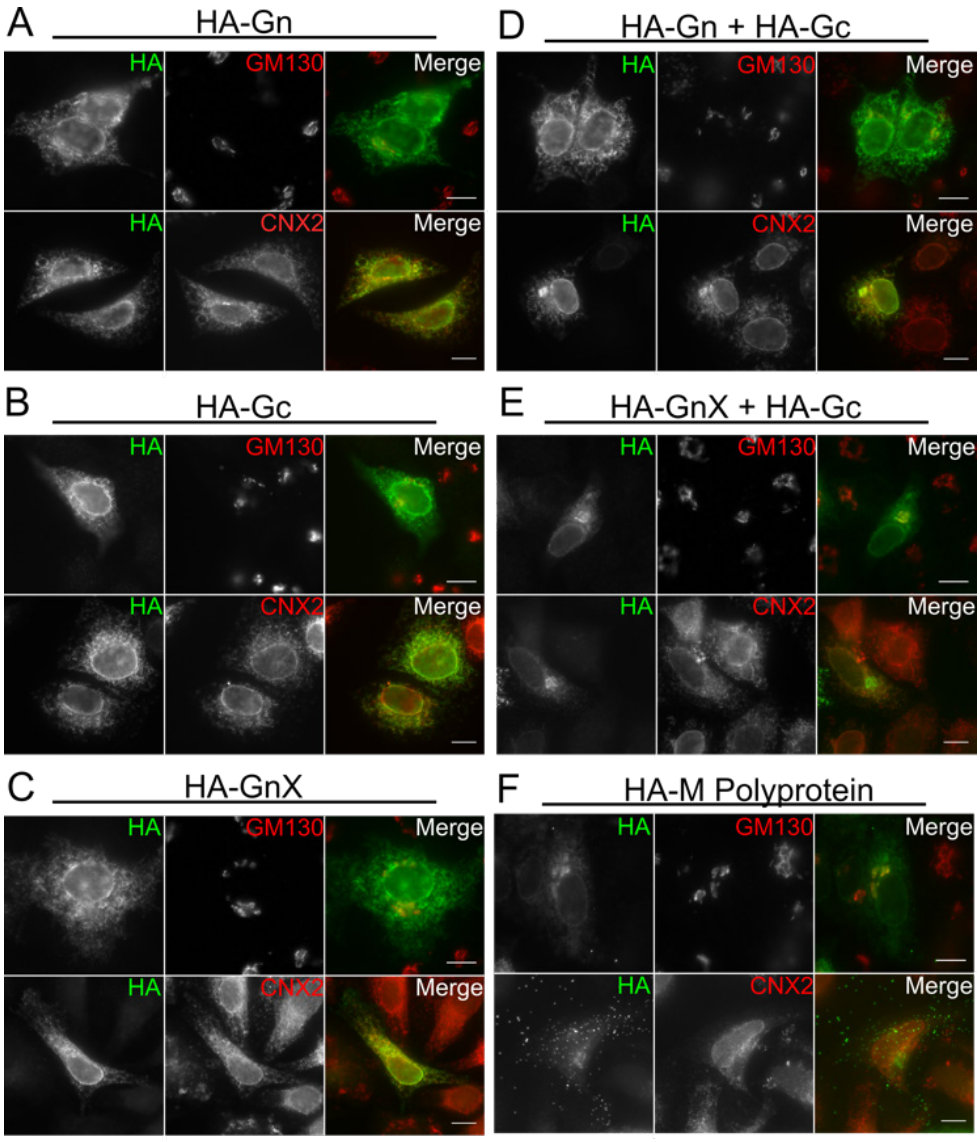

Figure 2. Intracellular localization of OROV glycoproteins. HeLa cells were transfected with plasmids expressing the HA-tagged OROV glycoproteins or the M polyprotein (as indicated). Cells were fixed and co-stained with rabbit anti-HA (AF488) and either mouse anti-GM130 (AF568) or mouse anti-CNX2 (AF568) antibodies before analysis using wide-field fluorescence microscopy. Bars = 10 μm.

Inhibition of the post-Golgi transport disrupts OROV glycoprotein secretion

The OROV assembly pathway involves the recruitment of the host ESCRT machinery to Golgi membranes for virus particle production (5). To further investigate the intracellular trafficking of the OROV M polyprotein, drugs that interfere with different cellular trafficking pathways were utilised. Golgi

transport was disrupted at two different steps: Brefeldin A was used to inhibit ER to Golgi transport, and monensin was used to block post-Golgi transport (26, 27). As some ESCRT components recognise partner proteins by interacting with ubiquitin, we also incubated cells with the proteasome inhibitor MG132, which depletes cellular mono-ubiquitin by preventing the recycling of ubiquitin that occurs when ubiquitylated proteins are degraded by the proteasome (28). HEK293T cells were transfected with HA-tagged OROV M and the culture medium was collected before and after drug treatment to monitor glycoprotein secretion. Secretion of OROV glycoproteins was strongly reduced in cells treated with MG132 and was completely disrupted in cells treated with monensin or brefeldin A (Fig. 3A). Interestingly, only treatment with monensin led to an increase of glycoprotein abundance in the treated cell lysates (Fig. 3A). Microscopic analysis of drug-treated HeLa cells (Fig. 3B) showed that brefeldin A caused dispersal of the *cis*-Golgi marker GM130 and prevented co-localisation of GM130 with the OROV glycoproteins. Conversely, monensin treatment led to an enlarged GM130-positive structure that strongly co-localised with the OROV glycoprotein HA signal. There was no obvious difference in the distribution in GM130 staining or its co-localisation with the OROV glycoprotein HA signal in cells mock-treated or treated with the proteasome inhibitor MG132. These results demonstrate that glycoprotein secretion is inhibited when the Golgi apparatus or ubiquitin/proteasome system are disrupted, and that treatment of cells with monensin causes accumulation of OROV glycoproteins at GM130 positive compartments.

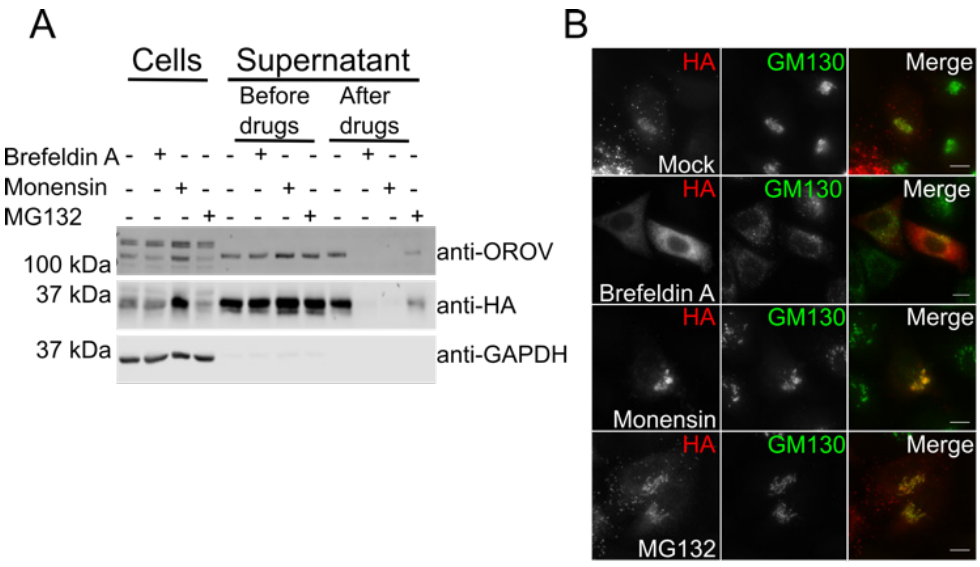

Figure 3. Disruption of the Golgi apparatus or proteasome prevents OROV VLP secretion. (A) HEK293T cells were transfected with HA-tagged OROV M polyprotein and after 18 h the cell supernatant was harvested and reserved. The culture medium was replenished and supplemented with the drugs brefeldin A, monensin or MG132, or with an equivalent amount of DMSO (mock). After 6h of drug treatment, cells and supernatant were harvested. All samples were then subjected to SDS-PAGE and immunoblotted using anti-HA and anti-OROV antibodies, with anti-GAPDH used as a loading control. (B) HeLa cells transfected and treated as (A). After drug treatment the cells were fixed and co-stained with rabbit anti-HA (AF568) and mouse anti-GM130 (AF488) antibodies before analysis using wide-field fluorescence microscopy. Bars = 10 μm.

Production of OROV VLPs requires ESCRT machinery

During OROV infection, multiple ESCRT components are recruited to Golgi membranes in order to promote virus particle production (5). VPS4 is a cellular ATPase that stimulates the disassembly of assembled ESCRT-III filaments at the necks of vesicles budding away from the cytoplasm, promoting membrane scission (9). VPS4 is recruited to Golgi membranes during OROV infection and the morphology of OROV viral factories is altered when infected cells express a dominant negative form of this enzyme (VPS4E/Q) that inhibits ESCRT-III disassembly (5). In order to analyse whether production of OROV VLPs is ESCRT-dependent, HEK293 cells stably expressing GFP-tagged wild-type or dominant negative VPS4 under the control of ecdysone response elements (29) were transfected with HA-tagged OROV M segment. Following transfection of these VPS4-expressing cells, or the parental HEK293 cells not expressing VPS4, the cells were treated with either ponasterone A (Pon A) to induce VPS4 expression, or with DMSO as a vehicle control, and the amount of secreted Gn and Gc was monitored by immunoblotting (Fig. 4A). The secretion of Gn and Gc by parental cells and those expressing wild-type GFP-VPS4 did not significantly differ when cells were treated with Pon A or DMSO (Fig 4B). Gn and Gc secretion was decreased when GFP-VPS4E/Q cells were treated with Pon A, although only the decrease in Gn was statistically significant (Fig. 4B). Similar to previous observations in OROV-infected HeLa cells (5), in Pon A treated cells OROV glycoproteins and GFP-tagged Vps4E/Q co-localised near to GM130-containing Golgi membranes (Fig. 4C). However, unlike previous studies of OROV-infected cells, we did not observe extensive co-localisation of GFP-tagged wild-type VPS4 with either the OROV glycoproteins nor the Golgi marker GM130.

To further investigate the interaction between ESCRT-III components and OROV glycoproteins, HeLa cells were transiently co-transfected with HA-tagged OROV M segment and dominant-negative C-terminally YFP/GFP tagged members of the charged multivesicular body protein (CHMP) family (30). Co-localization could clearly be observed between OROV glycoproteins and CHMP6-YFP, CHMP4A-YFP, CHMP4B-YFP, CHMP2A-YFP or CHMP1A-YFP (Fig. 4D). These co-localised proteins were near to GM130-positive Golgi membranes, although the overlap between the HA/YFP and GM130 signals was not extensive (Fig. 4D). In contrast, there was no apparent co-localization between OROV glycoproteins and CHMP2B-GFP or CHMP3-YFP (Fig. 4D). These data show that multiple ESCRT-III components associate with OROV glycoproteins and suggest that ESCRT-III activity is required for efficient VLP formation, as has been observed for production of OROV virus particles in infected cells.

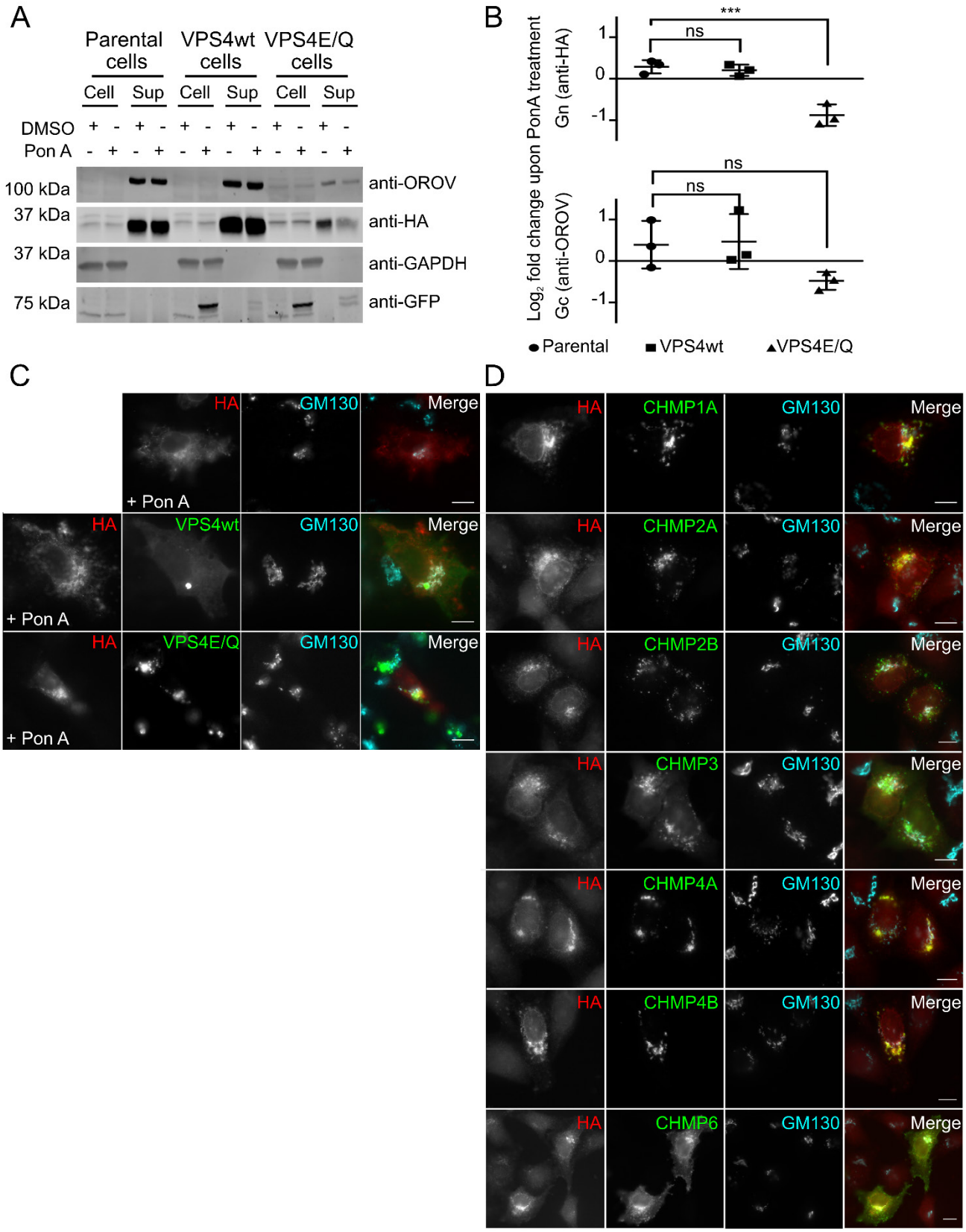

Figure 4. Interaction of OROV glycoproteins with cellular ESCRT machinery. (A) HEK293 cells stably expressing GFP-tagged wild-type VPS4 (VPS4wt) or a dominant negative mutant (VPS4E/Q) under the control of the ecdysone response element, or parental cells as a control, were transfected with HA-M segment and treated with either 1 μM ponasterone A (Pon A) or with DMSO as a control.

After 48 h, cells (*Cell*) and supernatant (*Sup*) were harvested, subjected to SDS-PAGE and immunoblotted using anti-GFP, anti-HA and anti-OROV antibodies, with anti-GAPDH used as a loading control. (B) Quantitation of fold change in Gn (anti-HA; upper panel) and Gc (anti-OROV; lower panel) secretion upon ponasterone A treatment. The $\log_2$ ratio of protein in the supernatant of ponasterone A-treated cells versus cells treated with DMSO is shown for three independent experiments. Bars represent the mean ± SD. ***, $p < 0.005$ (One-way ANOVA using Dunnett's test for multiple comparisons to parental control cells). (C) HEK293 cells expressing GFP-VPS4wt or GFP-VPS4E/Q, or parental cells, were transfected with HA-tagged OROV M segment and treated with 1 μM ponasterone A for 18 h before being fixed and co-stained with rabbit anti-HA (AF568) and mouse anti-GM130 (AF647) antibodies and then analysed by wide-field fluorescence microscopy. Bars = 10 μm. (D) HeLa cells were co-transfected with plasmids expressing HA-tagged OROV M segment and YFP/GFP-tagged ESCRT-III components (as indicated). After 18 h, cells were fixed and co-stained with rabbit anti-HA (AF568) and mouse anti-GM130 (AF647) before being analysed by wide-field fluorescence microscopy. Bars = 10 μm.

Discussion

In this present work we have characterized the production of Oropouche virus-like particles (VLPs) as a tool to study OROV assembly and budding. It has been reported for other members of the order *Bunyavirales* that the surface glycoproteins are the main viral components necessary for VLP production (19, 20). Here, we showed that OROV VLPs are formed when Gn and Gc are co-expressed, with the proteolytic processing of OROV Gn differing from that of other orthobunyaviruses, that VLP production is inhibited by drugs that interfere with Golgi or proteasome function, and that the cellular ESCRT machinery is required for efficient VLP production.

Previous studies of BUNV have shown two cleavage sites between the boundaries of Gn and NSm in the M polyprotein, either side of the second TMD (23). Specifically, Shi and colleagues (23) observed that the second TMD of the BUNV M polyprotein (which they term NSm^{SP}) acts as a signal peptide for NSm, being cleaved at its C terminus by cellular signal peptidases, and that this TMD is subsequently liberated from the mature Gn protein by signal peptide peptidase. In contrast, we show that this second TMD (which we term X) is retained by the mature OROV Gn protein. Shi and colleagues (23) also observed that the migration of the BUNV Gn protein in SDS-PAGE changed linearly when Gn was truncated before the start of the second TMD. However, when stop codons were introduced at or following the start of this second TMD the resultant Gn protein migrated identically to mature Gn protein arising from BUNV infection or M polyprotein expression. In contrast, we observe that the migration of HA-tagged Gn OROV (residues 1–313), containing only one TMD, differs from that of HA-tagged Gn obtained when the entire OROV M polyprotein is expressed (Fig 1B, C). However, the migration of HA-tagged GnX (residues 1–339) matched that of the mature HA-tagged Gn protein obtained via M polyprotein processing (Fig 1C). Furthermore, we observe the efficient secretion of OROV glycoproteins into the culture medium, presumably as VLPs, when GnX (residues 1–339) is co-expressed with Gc or when the OROV M segment is expressed as a single polyprotein, but not when Gn (residues 1–313) is co-expressed with Gc. Taken together, these data show that a mature Gn protein spanning two TMDs (GnX) is produced when the OROV M polyprotein is processed, in contrast to previous observations for BUNV, and we conclude that the requirement for cleavage of the second TMD from Gn by signal peptide peptidase differs across orthobunyaviruses.

In addition to differences in proteolytic processing of the M polypeptide between BUNV and OROV, we observed a difference in the requirement for co-expression of Gn and Gc in order for these proteins to traffic from the ER to the Golgi. Previous studies have shown that the Gn protein of BUNV is trafficked to the Golgi complex when expressed alone (7), due to the Golgi retention signal located on its first TMD (31). In contrast, we observe that neither Gn with either one or two TMDs (Gn and GnX, respectively) nor Gc localise to the Golgi when expressed in isolation (Fig. 2). When Gc was co-expressed with Gn (one TMD), both proteins were still retained in the ER, whereas co-expression of Gc with GnX (two TMDs) resulted in strong co-localisation of the glycoproteins with the Golgi marker GM130. We observed similar co-localisation of the OROV glycoproteins with GM130 when expressing the entire M polyprotein. Taken together, these results confirm the requirement of the second Gn TMD for correct protein function. The difference in requirement for Gn and Gc co-expression in order to mature beyond the ER into the Golgi may highlight structural differences between the orthobunyavirus glycoproteins, with the BUNV Gn extracellular domain being capable of folding independently whereas the OROV Gn extracellular region requires Gc for folding and/or stabilisation.

Since Bunyavirus do not possess a matrix protein, the cytosolic tails of Gn and Gc are believed to be important for virus assembly and budding. The Gn cytosolic domain of Uukuniemi phlebovirus interacts with the virus ribonucleoprotein, which is crucial for genome packaging (32), and previous studies of BUNV showed the Gn and Gc cytosolic tails to be required for Golgi complex targeting, virus assembly and infectivity (33). Furthermore, it has been shown that the first TMD of BUNV Gn is required for correct Golgi targeting of Gc (31). We therefore investigated whether the Gn cytosolic tail (GnCTX) could serve as a chaperone for Gc. We observed that Gc is not secreted into the medium when co-expressed with GnCTX, suggesting that VLPs were not being correctly formed, whereas co-expression of Gc with GnX did promote glycoprotein secretion (Fig 1C). This data confirms that the Gn extracellular domain is required for secretion of Gc, consistent with previous studies of BUNV showing that mutations in the glycosylation sites of Gn prevented correct folding of both Gn and Gc (34).

Previous studies of BUNV showed that budding and initial maturation steps occur in the Golgi stacks, but that full virus maturation does not proceed without a functional *trans*-Golgi (6). Fragmentation of the Golgi is observed when Vero cells are infected with BUNV, although these fragmented Golgi are still competent to sustain infectious virion production (6). Similarly, OROV infection leads to *trans*-Golgi network fragmentation as detected by dispersion of the TGN46 marker (5). We do not observe fragmentation of the Golgi in cells expressing the M polyprotein (Fig. 2F and 3B), suggesting that additional OROV proteins are required to promote Golgi fragmentation. In order to investigate the intracellular trafficking of OROV VLPs, we used two drugs that interfere with the Golgi complex in different manners. The drug monensin strongly disrupts *trans*-Golgi network function by altering the pH (27), allowing us to probe post-Golgi transport of VLPs (Figure 3). We observed an accumulation of glycoproteins at GM130-positive compartments in monensin-treated cells with a concomitant drop in glycoprotein secretion into the extracellular medium, confirming that a functional *trans*-Golgi network is required for OROV VLP secretion. Brefeldin A prevents protein traffic from the ER to the Golgi but allows retrograde trafficking to proceed, causing re-adsorption of the Golgi into the ER (35). As

331 expected, we observed a loss of the distinct Golgi-like staining patterns for both the OROV glycoproteins
332 and the *cis*-Golgi marker GM130, plus a loss of VLP secretion, following brefeldin A treatment.
333 Interestingly, we do not observe accumulation of intracellular glycoproteins, consistent with a loss in
334 protein translation caused by the ER stress induced by brefeldin A treatment (36). Taken together, our
335 data show that disruption of Golgi function inhibits OROV VLPs production, as has been observed
336 previously for cells infected with BUNV (37).

337 The production of OROV infectious particles requires the cellular ESCRT machinery (5). To probe
338 whether OROV VLP production also requires ESCRT activity, and thus faithfully recapitulates infectious
339 virus particle production, we investigated the association of ESCRT components with OROV
340 glycoproteins and the requirement of ESCRT machinery for VLP production. Exploitation of the cellular
341 ESCRT machinery by retroviruses requires the small protein ubiquitin (13), with retrovirus budding
342 being inhibited when free ubiquitin is depleted from cells by means of proteasomal inhibition (38). We
343 observe that secretion of OROV VLPs is strongly reduced in cells treated with the proteasomal inhibitor
344 MG132 (Fig. 3), consistent with a role for ubiquitin and the ESCRT machinery in VLP secretion. The
345 ESCRT-III–disassembling ATPase VPS4 has previously been shown to co-localise with OROV
346 replication sites, with expression of the ATPase-defective VPS4E/Q mutant leading to changes in
347 replication compartment morphology (5). We observe that the secretion of OROV VLPs is decreased
348 from cells expressing VPS4E/Q, whereas secretion from parental cells or those expressing wild-type
349 VPS4 is unchanged (Fig. 4A, B). This decrease in secretion is statistically significant when quantitating
350 HA-tagged Gn ($p = 0.0006$), whereas there is a consistent but not statistically significant decrease when
351 quantitating Gc using anti-OROV ($p = 0.1451$). We are unable to explain this discrepancy except to
352 note that the anti-HA staining of Gn was more consistent across experiments than the anti-OROV
353 staining of Gc, potentially due to higher detection efficiency afforded by the monoclonal anti-HA
354 antibody or more consistent electrophoretic transfer of the smaller Gn protein to nitrocellulose
355 membranes. We also note that glycoprotein secretion was generally poorer in unstimulated VPS4E/Q
356 expressing cells (Fig 4A), potentially due to an undetectable level of 'leaky' expression of the VPS4E/Q
357 mutant in unstimulated cells that would reduce the dynamic range afforded by this assay. Interestingly,
358 while GFP-VPS4E/Q co-localized with OROV glycoproteins at Golgi membranes in a similar manner
359 as OROV infectious particles (5), GFP-VPS4wt did not (Fig. 4). This suggests that additional OROV
360 proteins are required for stable recruitment of VPS4 to OROV glycoproteins.

361 To further understand how cellular ESCRT components may promote OROV VLP production, we
362 investigated the co-localisation of OROV glycoproteins with overexpressed, dominant-negative
363 YFP/GFP-tagged cellular ESCRT-III components. CHMP6, a component known to initiate ESCRT-III
364 polymers (8), co-localises with OROV glycoproteins, as do the polymerising ESCRT-III components
365 CHMP2A and all isoforms of CHMP4 (Fig. 4). However, we don't observe co-localisation of CHMP2B
366 (Fig. 4). CHMP2B displays affinity for $PI(4,5)P_2$ and is known to be required for formation of long-lived
367 ESCRT-III complexes involved in the morphogenesis and maintenance of dendritic spines (39). Both
368 CHMP2A and CHMP2B can contribute to HIV-1 budding, with loss of both leading to severe defects in
369 virus assembly (40). On face value, our data suggest that OROV VLP production is likely to depend

more strongly on CHMP2A rather than CHMP2B. However, CHMP3 was not observed to co-localise with OROV glycoproteins (Fig. 4D) and previous experiments with HIV suggest that CHMP2A-mediated stimulation of virus budding requires CHMP3 (11). Further experiments will be required in order to determine which CHMP2 isoform stimulates OROV budding, and whether CHMP3 participates in this activity.

In summary, we have demonstrated that OROV Gn contains two transmembrane domains essential for OROV glycoprotein trafficking to the Golgi complex. Pharmacological disruption of Golgi function inhibits OROV VLP secretion, as does perturbation of ESCRT complex function. Furthermore, we observe co-localisation of only selected CHMP-family ESCRT-III components with the OROV glycoproteins, giving initial insights into the cellular requirements for virus budding. We anticipate that our OROV VLP production assay will facilitate future studies on bunyavirus assembly and budding, and accelerate attempts to develop vaccines against OROV and/or identifying novel antiviral drugs that prevent Oropouche fever.

Materials and Methods

Cell Culture

Mycoplasma-free HeLa and HEK293T cells were maintained in Dulbeco's modified Eagle's medium (DMEM; Gibco) supplemented with 10% heat-inactivated foetal calf serum and 2 mM glutamine at 37°C in a humidified 5% CO_2 atmosphere. HEK293 cells stably expressing the ecdysone receptor (EcR-293; Invitrogen), and derived cell lines stably expressing GFP-tagged wild-type or dominant negative VPS4 under the control of ecdysone response elements, were maintained in the medium listed above supplemented with 400 µg/ml Zeocin and 800 µg/ml G418 (29).

Plasmids and Constructs

All fragments of the M polyprotein from OROV strain BeAn19991 (GenBank ID KP052851.1) used in this study were synthesised (GeneArt) following codon-optimization for expression in human cells. Constructs encoding Gn (M polyprotein residues 1–313) and Gc (residues 482–1420) were synthesised with an HA epitope tag and BamHI restriction sequence immediately following the Gn signal sequence (SS), and were cloned into pcDNA3.1(+) using the restriction enzymes NheI and XhoI. To generate the HA-tagged OROV M polypeptide construct, an extended NSm fragment (M polyprotein residues 299–496) was synthesised to overlap with the N and C termini of Gc and Gn, respectively. The sequences for Gc, NSm and the entire pcDNA3.1 vector encoding Gn with an N-terminal signal sequence plus HA tag were amplified by PCR using KOD Hot Start DNA polymerase (Novagen) using the primers shown in Table 1, mixed and then concatenated using the NEBuilder HiFi assembly kit according to the manufacturer's instructions to yield pSnH-OROV-M. HA-tagged GnX was generated by site directed mutagenesis of pSnH-OROV-M to insert a stop codon after residue 339 using the mutagenic primers listed in Table 1. HA-tagged GnCTX was amplified from pSnH-OROV-M using the primers shown in Table 1, digested with the restriction endonucleases BamHI and XhoI, and ligated into BamHI/XhoI

406 digested pSnH-OROV-M to yield the Gn signal sequence and an HA epitope tag followed by M
407 polypeptide residues 203–339. All expression constructs were verified by Sanger sequencing. CHMP-
408 YFP/GFP plasmids were as described previously (30).

409 *Table 1. Oligonucleotide primers used in this study. Restriction sites are in **bold**.*

Name	Sequence (5′ to 3′)	Details
Gn C-terminal forward	CAAGAGCCTGAGCAAGGCCAG	Amplify NSm to generate HA-M polyprotein construct
Gc N-terminal reverse	CTTGGTAGGTGATCTTGATGTCCTTGC	Amplify NSm to generate HA-M polyprotein construct
pcDNA 3′ forward	CGTTTAAACCCGCTGATCAGC	Amplify Gn and pcDNA vector to generate HA-M polyprotein construct
Gn C-terminal reverse	GCTCTTGCTCTTGCACATCTGTC	Amplify Gn and pcDNA vector to generate HA-M polyprotein construct
Gc N-terminal forward	GATGAGGACTGCCTGAGCAAGGAC	Amplify Gc to generate HA-M polyprotein construct
BGH reverse	TAGAAGGCACAGTCGAGG	Amplify Gc to generate HA-M polyprotein construct
GnX forward	CGAGCGGATGTACTAGCTGGAAGAACTG	Generate GnX by replacing reside 340 of HA-M polyprotein with a stop codon
GnX reverse	CAGTTCTTCCAGCTAGTACATCCGCTCG	Generate GnX by replacing reside 340 of HA-M polyprotein with a stop codon
GnCTX forward	GAA**GGATCC**GAGGCTATGTGCGTGAACATC	Clone HA-tagged GnCTX
GnCTX reverse	GGAA**CTCGAG**TCAGTACATCCGCTCGCCGGC AATG	Clone HA-tagged GnCTX

410

411 *Antibodies*

412 For immunoblot analyses the following primary antibodies (identifier, dilution) were used: anti-GFP
413 (Sigma G2544, 1:5000), anti-OROV (Gc detection; ATCC VR-1228AF, 1:1000), anti-HA (Cell Signaling
414 Technology C29F4, 1:2000), anti-GAPDH (GeneTex GTX28245, 1:10000) and anti-EEA1 (AbCam
415 Ab2900, 1:1000). The secondary antibodies were LI-COR IRDye 680T conjugated donkey anti-rabbit
416 (926-68023) or goat anti-mouse (926- 68020), or LI-COR IRDye 800CW conjugated donkey anti-rabbit
417 (926-32213) or goat anti-mouse (926-32210). For immunocytochemistry the following primary
418 antibodies (identifier, dilution) were used: anti-HA (Cell Signaling Technology, 1:1000), anti-GM130 (BD
419 Biosciences 610822, 1:1000) and anti-Calnexin2 (BD Biosciences 610523, 1:100). Secondary
420 antibodies were Alexa Fluor conjugated goat anti-mouse (A-21236, A-11001 and A-11031,
421 ThermoFisher), donkey anti-rabbit (A-10042, ThermoFisher) and goat anti-rabbit (A-11008,
422 ThermoFisher).

OROV VLP assay and immunoblotting

HEK293T cells were seeded at 2.5×10^5 cells per well in six well dishes. Cells were transfected by mixing 2 µg of DNA (split evenly by mass between the plasmids indicated) and 1.5 µg of branched polyethylenimine (PEI; average MW ~25,000, Merck) in Opti-MEM (ThermoFisher), incubating at room temperature for 20 min and then applying to cells. Cell culture medium was harvested after 48 h and cleared of cellular debris by centrifugation at 800×g for 10 min at 4°C. Virus-like particles (VLPs) in the supernatants were pelleted by centrifugation at 100,000×g at 4°C for 90 min using a TLA-55 rotor (Beckman). The resultant pellets, containing VLPs, were resuspended and boiled in sodium dodecyl sulfate-polyacrylamide gel electrophoresis (SDS-PAGE) sample buffer. Cell samples were harvested by centrifugation and resuspended in lysis buffer (50 mM Tris pH 7.9, 150 mM NaCl, 1% (v/v) IGEPAL CA-630 (a.k.a. NP-40), 1% (w/v) sodium deoxycholate) supplemented with protease inhibitor cocktail (Roche) and incubated on ice for 30 min. Lysates were clarified by centrifugation at 20,000×g for 10 min at 4°C. The protein concentration in each lysate sample was normalized following quantification using the BCA assay (ThermoFisher) and samples were boiled in SDS-PAGE sample buffer. Samples were separated by SDS-PAGE using 10% or 15% (w/v) polyacrylamide gels and transferred to Protran nitrocellulose membranes (Perkin Elmer) using the Mini-Trans blot system (BioRad) following the manufacturer's protocol. After blocking in PBS with 5% (w/v) non-fat milk powder, membranes were incubated with primary antibody at room temperature for 1 h or overnight at 4°C, washed, and then incubated with the secondary antibody for 1 h at room temperature. Dried blots were visualized on an Odyssey CLx infrared scanner (LI-COR).

For VLP isolation following drug treatment, HEK293T cells were transfected with a plasmid expressing HA-tagged M polyprotein as described above. After 18 h, the culture medium was collected and VLPs were isolated by ultracentrifugation as described above ("Before drugs"). The medium was replaced with FreeStyle 293 medium (ThermoFisher) supplemented with brefeldin A (5 µg/mL), monensin (1 µM), or MG132 (10 µM), and cells were incubated for a further 6 h before the supernatant and cell lysates were harvested and processed as described above ("After drugs").

For VLP isolation from ecdysone-responsive stable cell lines, cells were seeded differently. Parental and GFP-VPS4wt EcR293 cells were seeded at 5×10^6 cells per 9 cm dish, whereas GFP-VPS4E/Q EcR293 cells (which grow more slowly) were seeded at 8×10^6 cells per 9 cm dish. Cells were transfected with 7.7 µg of a plasmid expressing HA-tagged M polyprotein using TransIT-LT1 (Mirus) and after 6 h the cells were treated with either DMSO or ponasterone A (1 µM). After 18 h of drug treatment, the medium was refreshed using FreeStyle 293 medium (ThermoFisher). Cell lysates and supernatants were harvested at 48 h post-transfection and processed as described above.

Immunocytochemistry

HeLa cells were seeded on glass coverslips at a density of 5×10^4 cells per well in 24 well dishes. Cells were transfected with 250 ng of DNA (split evenly by mass between the plasmids indicated) using

TransIT-LT1 (Mirus) and incubated for 24 h before being transferred onto ice. Cells were washed with ice-cold PBS and fixed with cold 250 mM HEPES pH 7.5, 4% (v/v) electron microscopy-grade formaldehyde (PFA, Polysciences) for 10 min on ice before and then incubated with 20 mM HEPES pH 7.5, 8% (v/v) PFA at room temperature for a further 20 min. After washing with PBS, cells were permeabilized by incubation with 0.1% saponin in PBS for 30 min before being incubated with blocking buffer (5% [v/v] FBS, 0.1% saponin in PBS) for 30 min. Primary antibodies were diluted in blocking buffer and incubated with coverslips for 2 h. Coverslips were washed five times with blocking buffer before incubation for 1 h with the relevant secondary antibodies diluted in blocking buffer. Coverslips were washed five times with blocking buffer, three times with 0.1% saponin in PBS, three times with PBS, and finally with ultrapure water. Coverslips were mounted using Mowiol 4-88 (Merck) containing 200 nM 4′,6-diamidino-2-phenylindole (DAPI) and allowed to set overnight. Cells were analyzed with an Olympus IX81 fluorescence microscope. Images were captured using a Reitga 2000R charge-coupled device camera and processed using Fiji ImageJ software (23).

For the drug treatment assay, HeLa cells were seeded on glass coverslips at a density of 5×10^4 cells per well in 24 well dishes and transfected with a plasmid expressing HA-tagged M polyprotein. After 18 h the culture medium was replaced and supplemented with brefeldin A (5 µg/mL), monensin (1 µM), or MG132 (10 µM). After 6 h of drug treatment, cells were fixed and processed as described above.

Ecdysone-responsive stable cell lines were seeded on poly-D-lysine treated glass coverslips at a density of 2×10^4 cells per well in 24 well dishes. Cells were transfected with 250 ng of a plasmid expressing HA-tagged M polyprotein using TransIT-LT1 (Mirus) and after 6 h cells were treated with ponasterone A (1 µM) or DMSO. After 18 h of drug treatment, cells were fixed and processed as described above.

Acknowledgements

The authors thank Susanna Colaco for superb technical assistance. This work was supported by doctoral studentship and travelling fellowship from the Fundação de Amparo à Pesquisa do Estado de São Paulo (FAPESP; 2016/18356-4 and 2019/02945-9) to NSB, by a FAPESP Pump Priming award (2019/02418-9) to LLPdS, by a Biotechnology and Biological Sciences Research Council (BBSRC)/FAPESP pump priming award (BB/S018670/1) to CMC, LLPdS and SCG, and by a Sir Henry Dale Fellowship co-funded by the Royal Society and the Wellcome Trust (098406/Z/12/B) to SCG.

References

1. Sakkas H, Bozidis P, Franks A, Papadopoulou C. 2018. Oropouche Fever: A Review. Viruses 10:175.
2. Romero-Alvarez D, Escobar LE. 2018. Oropouche fever, an emergent disease from the Americas. Microbes Infect 20:135-146.
3. Gutierrez B, Wise EL, Pullan ST, Logue CH, Bowden TA, Escalera-Zamudio M, Trueba G, Nunes MRT, Faria NR, Pybus OG. 2020. Evolutionary Dynamics of Oropouche Virus in South America. J Virol 94:e01127-19.
4. Elliott RM. 2014. Orthobunyaviruses: recent genetic and structural insights. Nat Rev Microbiol 12:673-85.
5. Barbosa NS, Mendonça LR, Dias MVS, Pontelli MC, da Silva EZM, Criado MF, da Silva-Januário ME, Schindler M, Jamur MC, Oliver C, Arruda E, daSilva LLP. 2018. ESCRT machinery components are required for Orthobunyavirus particle production in Golgi compartments. PLoS Pathog 14:e1007047.
6. Salanueva IJ, Novoa RR, Cabezas P, López-Iglesias C, Carrascosa JL, Elliott RM, Risco C. 2003. Polymorphism and structural maturation of bunyamwera virus in Golgi and post-Golgi compartments. J Virol 77:1368-81.
7. Lappin DF, Nakitare GW, Palfreyman JW, Elliott RM. 1994. Localization of Bunyamwera bunyavirus G1 glycoprotein to the Golgi requires association with G2 but not with NSm. J Gen Virol 75:3441-51.
8. Christ L, Raiborg C, Wenzel EM, Campsteijn C, Stenmark H. 2017. Cellular Functions and Molecular Mechanisms of the ESCRT Membrane-Scission Machinery. Trends Biochem Sci 42:42-56.
9. Maity S, Caillat C, Miguet N, Sulbaran G, Effantin G, Schoehn G, Roos WH, Weissenhorn W. 2019. VPS4 triggers constriction and cleavage of ESCRT-III helical filaments. Sci Adv 5:eaau7198.
10. Schöneberg J, Pavlin MR, Yan S, Righini M, Lee IH, Carlson LA, Bahrami AH, Goldman DH, Ren X, Hummer G, Bustamante C, Hurley JH. 2018. ATP-dependent force generation and membrane scission by ESCRT-III and Vps4. Science 362:1423-1428.
11. Effantin G, Dordor A, Sandrin V, Martinelli N, Sundquist WI, Schoehn G, Weissenhorn W. 2013. ESCRT-III CHMP2A and CHMP3 form variable helical polymers in vitro and act synergistically during HIV-1 budding. Cell Microbiol 15:213-26.
12. Freed EO. 2002. Viral late domains. J Virol 76:4679-87.
13. Votteler J, Sundquist WI. 2013. Virus budding and the ESCRT pathway. Cell Host Microbe 14:232-41.
14. Tabata K, Arimoto M, Arakawa M, Nara A, Saito K, Omori H, Arai A, Ishikawa T, Konishi E, Suzuki R, Matsuura Y, Morita E. 2016. Unique Requirement for ESCRT Factors in Flavivirus Particle Formation on the Endoplasmic Reticulum. Cell Rep 16:2339-47.
15. Vietri M, Radulovic M, Stenmark H. 2020. The many functions of ESCRTs. Nat Rev Mol Cell Biol 21:25-42.
16. Watanabe S, Watanabe T, Noda T, Takada A, Feldmann H, Jasenosky LD, Kawaoka Y. 2004. Production of novel Ebola virus-like particles from cDNAs: an alternative to Ebola virus generation by reverse genetics. J Virol 78:999-1005.
17. Strecker T, Eichler R, Meulen J, Weissenhorn W, Dieter Klenk H, Garten W, Lenz O. 2003. Lassa virus Z protein is a matrix protein and sufficient for the release of virus-like particles. J Virol 77:10700-5.
18. Roldão A, Mellado MC, Castilho LR, Carrondo MJ, Alves PM. 2010. Virus-like particles in vaccine development. Expert Rev Vaccines 9:1149-76.
19. Acuña R, Cifuentes-Muñoz N, Márquez CL, Bulling M, Klingström J, Mancini R, Lozach PY, Tischler ND. 2014. Hantavirus Gn and Gc glycoproteins self-assemble into virus-like particles. J Virol 88:2344-8.
20. Overby AK, Popov V, Neve EP, Pettersson RF. 2006. Generation and analysis of infectious virus-like particles of uukuniemi virus (bunyaviridae): a useful system for studying bunyaviral packaging and budding. J Virol 80:10428-35.

21. Acrani GO, Tilston-Lunel NL, Spiegel M, Weidmann M, Dilcher M, Andrade da Silva DE, Nunes MR, Elliott RM. 2015. Establishment of a minigenome system for Oropouche virus reveals the S genome segment to be significantly longer than reported previously. J Gen Virol 96:513-23.
22. Kohl A, Hart TJ, Noonan C, Royall E, Roberts LO, Elliott RM. 2004. A bunyamwera virus minireplicon system in mosquito cells. J Virol 78:5679-85.
23. Shi X, Botting CH, Li P, Niglas M, Brennan B, Shirran SL, Szemiel AM, Elliott RM. 2016. Bunyamwera orthobunyavirus glycoprotein precursor is processed by cellular signal peptidase and signal peptide peptidase. Proc Natl Acad Sci U S A 113:8825-30.
24. Tilston-Lunel NL, Acrani GO, Randall RE, Elliott RM. 2015. Generation of Recombinant Oropouche Viruses Lacking the Nonstructural Protein NSm or NSs. J Virol 90:2616-27.
25. Nielsen H. 2017. Predicting Secretory Proteins with SignalP. Methods Mol Biol 1611:59-73.
26. Fujiwara T, Oda K, Yokota S, Takatsuki A, Ikehara Y. 1988. Brefeldin A causes disassembly of the Golgi complex and accumulation of secretory proteins in the endoplasmic reticulum. J Biol Chem 263:18545-52.
27. Mollenhauer HH, Morré DJ, Rowe LD. 1990. Alteration of intracellular traffic by monensin; mechanism, specificity and relationship to toxicity. Biochim Biophys Acta 1031:225-46.
28. Mimnaugh EG, Chen HY, Davie JR, Celis JE, Neckers L. 1997. Rapid deubiquitination of nucleosomal histones in human tumor cells caused by proteasome inhibitors and stress response inducers: effects on replication, transcription, translation, and the cellular stress response. Biochemistry 36:14418-29.
29. Crump CM, Yates C, Minson T. 2007. Herpes simplex virus type 1 cytoplasmic envelopment requires functional Vps4. J Virol 81:7380-7.
30. Pawliczek T, Crump CM. 2009. Herpes simplex virus type 1 production requires a functional ESCRT-III complex but is independent of TSG101 and ALIX expression. J Virol 83:11254-64.
31. Shi X, Lappin DF, Elliott RM. 2004. Mapping the Golgi targeting and retention signal of Bunyamwera virus glycoproteins. J Virol 78:10793-802.
32. Overby AK, Pettersson RF, Neve EP. 2007. The glycoprotein cytoplasmic tail of Uukuniemi virus (Bunyaviridae) interacts with ribonucleoproteins and is critical for genome packaging. J Virol 81:3198-205.
33. Shi X, Kohl A, Li P, Elliott RM. 2007. Role of the cytoplasmic tail domains of Bunyamwera orthobunyavirus glycoproteins Gn and Gc in virus assembly and morphogenesis. J Virol 81:10151-60.
34. Shi X, Brauburger K, Elliott RM. 2005. Role of N-linked glycans on bunyamwera virus glycoproteins in intracellular trafficking, protein folding, and virus infectivity. J Virol 79:13725-34.
35. Sciaky N, Presley J, Smith C, Zaal KJ, Cole N, Moreira JE, Terasaki M, Siggia E, Lippincott-Schwartz J. 1997. Golgi tubule traffic and the effects of brefeldin A visualized in living cells. J Cell Biol 139:1137-55.
36. Kaufman RJ. 1999. Stress signaling from the lumen of the endoplasmic reticulum: coordination of gene transcriptional and translational controls. Genes Dev 13:1211-33.
37. Novoa RR, Calderita G, Cabezas P, Elliott RM, Risco C. 2005. Key Golgi factors for structural and functional maturation of bunyamwera virus. J Virol 79:10852-63.
38. Patnaik A, Chau V, Wills JW. 2000. Ubiquitin is part of the retrovirus budding machinery. Proc Natl Acad Sci U S A 97:13069-74.
39. De Franceschi N, Alqabandi M, Miguet N, Caillat C, Mangenot S, Weissenhorn W, Bassereau P. 2018. The ESCRT protein CHMP2B acts as a diffusion barrier on reconstituted membrane necks. J Cell Sci 132.
40. Morita E, Sandrin V, McCullough J, Katsuyama A, Baci Hamilton I, Sundquist WI. 2011. ESCRT-III protein requirements for HIV-1 budding. Cell Host Microbe 9:235-242.